ELSEVIER

Chemical Engineering Journal 131 (2007) 195–201

Chemical Engineering Journal

www.elsevier.com/locate/cej

Effect of composition on the formation of poly(DL-lactide) microspheres for drug delivery systems: Mesoscale simulations

Xindong Guo, Lijuan Zhang, Yu Qian *, Jian Zhou

School of Chemical Engineering, South China University of Technology, Guangzhou 510640, PR China

Received 29 June 2006; received in revised form 3 January 2007; accepted 7 January 2007

Abstract

In this work, the structure–property relationship of drug delivery systems (DDS) is investigated by dissipative particle dynamics (DPD) simulations. Nifedipine is selected as the model drug, whereas poly(DL-lactide) (PLA) as the carrier and polyvinyl alcohol (PVA) as the stabilizer. It is shown from DPD simulations that PLA, drug, and PVA could aggregate and form microspheres under a defined composition recipe; drug molecules are amorphously and homogeneously distributed inside the carrier matrix, on whose surface the stabilizer PVA molecules are adsorbed. Under different compositions of each component, aggregate morphologies of the oil phase are observed as spherical, columnar, and lamellar structures. A phase diagram of DDS has been proposed, which could be used to guide the experimental preparation of DDS with desired properties.

Keywords: Dissipative particle dynamics; Mesoscale simulation; Drug delivery; Controlled release; Poly-lactide

1. Introduction

Over the past decade, studies on drug delivery systems (DDS) have been improved considerably [1–3], resulting in a precisely controlled and sustained drug release rate over prolonged time. Coupling drugs to a polymer matrix [4–6] offers an intelligent approach to develop DDS for the efficient carrier characteristics of polymers. Based on their long and safe history of use as biodegradable materials, polymer drug carriers have been considered important for enhanced drug stability and increased drug solubility, and have been widely employed for the controlled release of drugs.

Polymer microspheres for controlled release have been extensively studied by experiments over the past decade [7–9]. The biodegradable poly(DL-lactide-*co*-glycolide) (PLGA) microspheres loaded with ibuprofen were developed and optimized by Carballido et al. [7], resulting in a long-term release of drug from 24 h up to 8 days. The release profiles of anti-cancer drugs, 5-fluorouracil and paclitaxel, were controlled over 2 weeks by being loaded into a matrix of four-armed block copolymers of 1-PLA and poly(ethylene oxide) (PEO) [8]. Two types of drug distributions in a microsphere have been prepared from the blending of PLA and PLGA by Matsumoto et al. [9]: one type with the drug-holding layer covered with the non-drug layer, while the other with the drug on the outer region of the microspheres. They [8] also studied the drug release mechanism of the first type. It is rather difficult for researchers to investigate the transformation of micro- or meso-structures of DDS by experiments. Thus, it is very important to study DDS with the help of computer simulations. Simulations in couple with experiments might provide deeper insights for the controlled preparation of DDS.

Dissipative particle dynamics (DPD), introduced by Hoogerbrugge and Koelman [10] in 1992, was used to simulate soft spherical beads interacting through a simple-wise potential, and thermally equilibrated through hydrodynamics [11]. In 1995, Español and Warren [12] pointed out that the total force acting on a particle is the sum of a conservative force, a dissipative force, and an additive random force. In 1997, Groot and Warren [13,14] made an important contribution on this method by establishing a relationship between a simple functional form of the conservative repulsion in DPD and the Flory–Huggins parameter theory, which lead DPD method widely applied in the study of mesostructures of complex systems [15–22]. Groot [15–17] studied polymer–surfactant aggregation, electrostatic interactions, and morphology change by using DPD method. Yuan et al. [18] drew the ternary phase diagram of AOT/water/iso-octane system using the results from DPD simulations. DPD is also used

* Corresponding author. Tel.: +86 20 87113046; fax: +86 20 87113046.
E-mail address: ceyuqian@scut.edu.cn (Y. Qian).

1385-8947/$ – see front matter © 2007 Elsevier B.V. All rights reserved.
doi:10.1016/j.cej.2007.01.013

to calculate the solubility parameter, surface tension [13,19], and the mean square end-to-end distance of polymer chain [20]. In addition, DPD simulation is also an efficient method to investigate the complex system consisting of polymer, surfactant, and water [21,22]. However, DPD has seldom been applied to the field of DDS.

In this work, DPD simulation technique is employed to investigate the effect of composition on aggregate morphologies of the drug-loaded microspheres. Nifedipine is selected as the model drug, whereas poly(DL-lactide) (PLA) as the carrier and polyvinyl alcohol (PVA) as the stabilizer. Effects of composition of each component on the formation of spherical aggregates will be investigated. This work will be helpful to understand the relationship of micro-structures and macro-performances of polymer microspheres for controlled release. A similar work on solid lipid microspheres (SLM) was also reported by our group recently [23]. The experimental analysis on this work is previously reported in detail by parts of the authors [24,25].

2. DPD simulations

2.1. DPD theory

An important concept of DPD simulation is the coarse-grained model, which means that a DPD bead represents a group of atoms or a volume of fluid that is large on the atomistic scale but still macroscopically small [26]. In DPD simulations, all beads comply with Newton's equations of motion [13,27]:

$$\frac{d\mathbf{r}_i}{dt} = \mathbf{v}_i, \qquad m_i \frac{d\mathbf{v}_i}{dt} = \mathbf{f}_i, \tag{1}$$

where $\mathbf{r}_i$, $\mathbf{v}_i$, m_i, and $\mathbf{f}_i$ are the position, velocity, mass, and force of bead i, respectively. Dimensionless units are used in DPD simulations usually, the mass of each bead is set to 1 DPD mass unit, resulting in an equation between the force acting on a bead and its acceleration [13]. The force acting on a bead is a sum of a conservative force ($\mathbf{F}_{ij}^{C}$), a dissipative force ($\mathbf{F}_{ij}^{D}$), and a random force ($\mathbf{F}_{ij}^{R}$) [12]:

$$\mathbf{f}_i = \sum_{j \neq i} (\mathbf{F}_{ij}^{C} + \mathbf{F}_{ij}^{D} + \mathbf{F}_{ij}^{R}), \tag{2}$$

where the sum runs over all other particles within a certain cutoff radius r_c, which is set to be 1 in simulations. The conservation force is a soft repulsion acting along the line of centers and is given by:

$$\mathbf{F}_{ij}^{C} = \begin{cases} a_{ij}(1 - r_{ij})\hat{\mathbf{r}}_{ij} & (r_{ij} < 1) \\ 0 & (r_{ij} \geq 1) \end{cases}, \tag{3}$$

where a_{ij} is a maximum repulsion between bead i and bead j; $\mathbf{r}_{ij} = \mathbf{r}_i - \mathbf{r}_j$, $r_{ij} = |\mathbf{r}_{ij}|$, $\hat{\mathbf{r}}_{ij} = \mathbf{r}_{ij}/|\mathbf{r}_{ij}|$. The other two forces are dissipative and random forces, which are given by:

$$\mathbf{F}_{ij}^{D} = -\frac{\sigma^2(\omega(r_{ij}))^2}{2kT}(\mathbf{v}_{ij} \cdot \hat{\mathbf{r}}_{ij})\hat{\mathbf{r}}_{ij}, \tag{4}$$

$$\mathbf{F}_{ij}^{R} = \frac{\sigma\omega(r_{ij})\hat{\mathbf{r}}_{ij}\zeta}{\sqrt{\delta_t}}, \tag{5}$$

where $\mathbf{v}_{ij} = \mathbf{v}_i - \mathbf{v}_j$, ζ is a random variable with zero mean and variance 1, δ_t is the time step used, the r-dependent weight function $\omega(r) = 1 - r$ for $r < 1$ and $\omega(r) = 0$ for $r > 1$.

In this study, a modified version of the velocity-Verlet algorithm has been used to integrate the Newton's equations [28]:

$$\begin{cases} \mathbf{r}_i(t + \Delta t) = \mathbf{r}_i(t) + \Delta t\mathbf{v}_i(t) + \frac{1}{2}(\Delta t)^2\mathbf{f}_i(t) \\ \tilde{\mathbf{v}}_i(t + \Delta t) = \mathbf{v}_i(t) + \lambda\,\Delta t\mathbf{f}_i(t) \\ \mathbf{f}_i(t + \Delta t) = \mathbf{f}_i(\mathbf{r}(t + \Delta t), \tilde{\mathbf{v}}(t + \Delta t)) \\ \mathbf{v}_i(t + \Delta t) = \mathbf{v}_i(t) + \frac{1}{2}\Delta t(\mathbf{f}_i(t) + \mathbf{f}_i(t + \Delta t)) \end{cases}, \tag{6}$$

where $\tilde{\mathbf{v}}(t + \Delta t)$ is the prediction of the velocity of a particle at time $t + \Delta t$. In this algorithm, the force is still updated once per integration, thus there is virtually no increase in computational cost.

2.2. Spring force

In the DPD model, atoms of each molecule are not directly represented, but they are grouped together into beads. Molecules are represented by several beads by a spring force to reproduce the typical nature of them. Groot and Warren [13] advocated the simple harmonic spring force on bead i:

$$\mathbf{F}_i^{S} = \sum_j C\mathbf{r}_{ij}, \tag{7}$$

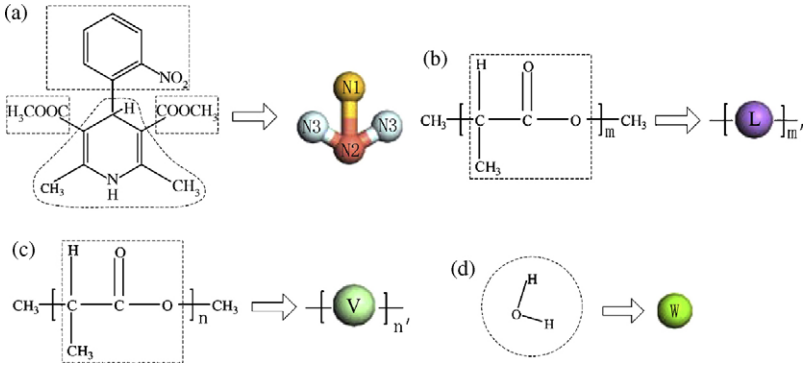

Fig. 1. Coarse-grained models of (a) nifedipine, (b) PLA, (c) PVA, and (d) water.

where C is the spring constant, and the mean distance between two consecutive chain beads is governed by the spring force and the repulsive interaction. The spring constant C is chosen so that, if all forces are considered, the average bead–bead distance along the chain has a reasonable value, which corresponds to the first peak in the bead–bead correlation function. In this study, the default value $C=4$ has been used, resulting in a slightly smaller distance for bonded beads than for non-bonded ones [14].

2.3. Models and simulation parameters used in DPD

Coarse-grained models of components are used in this study, as shown in Fig. 1. Each bead is represented by several atoms, which are closed by dashed lines. The nifedipine molecule is divided into three types of beads, named N1, N2, N3, respectively. Each monomer of PLA and PVA is considered as one bead named L and V, respectively. One molecule of water is represented as a bead W.

In order to calculate the conservation force, repulsion parameters a_{ij} between any two beads should be calculated. The repulsion parameters between beads of the same type, a_{ii}, are chosen according to [14]:

$$a_{ii}\rho = 75k_{\mathrm{B}}T, \tag{8}$$

where k_{B} is the Boltzmann constant and T is the system temperature. The bead density $\rho=3$ has been used in a previous work [14], and $k_{\mathrm{B}}T=1$ has been used [10]. Repulsion parameters between different types of beads are linearly related with the Flory–Huggins parameters (χ_{ij}) according to:

$$a_{ij} = a_{ii} + 3.27\chi_{ij}, \tag{9}$$

χ_{ij} can be calculated from solubility parameters [19]:

$$\chi_{ij} = \frac{V_{\mathrm{bead}}}{kT}(\delta_i - \delta_j)^2, \tag{10}$$

where V_{bead} is the arithmetic average of molar volumes of two beads; δ_i and δ_j are the solubility parameters of bead i and j, which can be obtained from experiments or molecular dynamics simulations. In this study, solubility parameters are calculated using Amorphous Cell and Discover modules in Materials Studio software (Accelrys Inc.) with the COMPASS force field.

By using Eqs. (8)–(10), DPD repulsion parameters are calculated. The parameters are listed in Table 1.

A $20\times20\times20$ R_{c}^3 (R_{c} is the DPD length unit or the cut-off radius) box was adopted. Periodic boundary conditions were applied in all three directions. In DPD simulations, each molecule of drug, PLA, PVA and water is coarse-grained into beads with the bead number of 4, 55, 70, and 1, respectively. The total number of beads, 24,000, was used in all simulations. In each DPD simulation, the dimensionless time step of 0.05 was employed. And 20,000 steps have been adopted to get a steady phase. The temperature was set constant at 308.15 K. All DPD simulations were performed by the Materials Studio software (Accelrys).

Table 1
The interaction parameters used in DPD simulations (unit: kT)

a_{ij}	L	N1	N2	N3	W	V
L	25					
N1	25.12	25				
N2	25.39	25.08	25			
N3	25.14	25.00	25.03	25		
W	69.62	69.5	69.0	59.19	25	
V	28.74	27.97	27.34	27.16	51	25

3. Results and discussion

3.1. The aggregate morphology of DDS

Several snapshots of configurations of the studied DDS during one DPD simulation are shown in Fig. 2. The system includes nifedipine, PLA, PVA, and water with the molar ratio of 38:5:1:956. To show aggregate morphologies clearly, water molecules are not displayed.

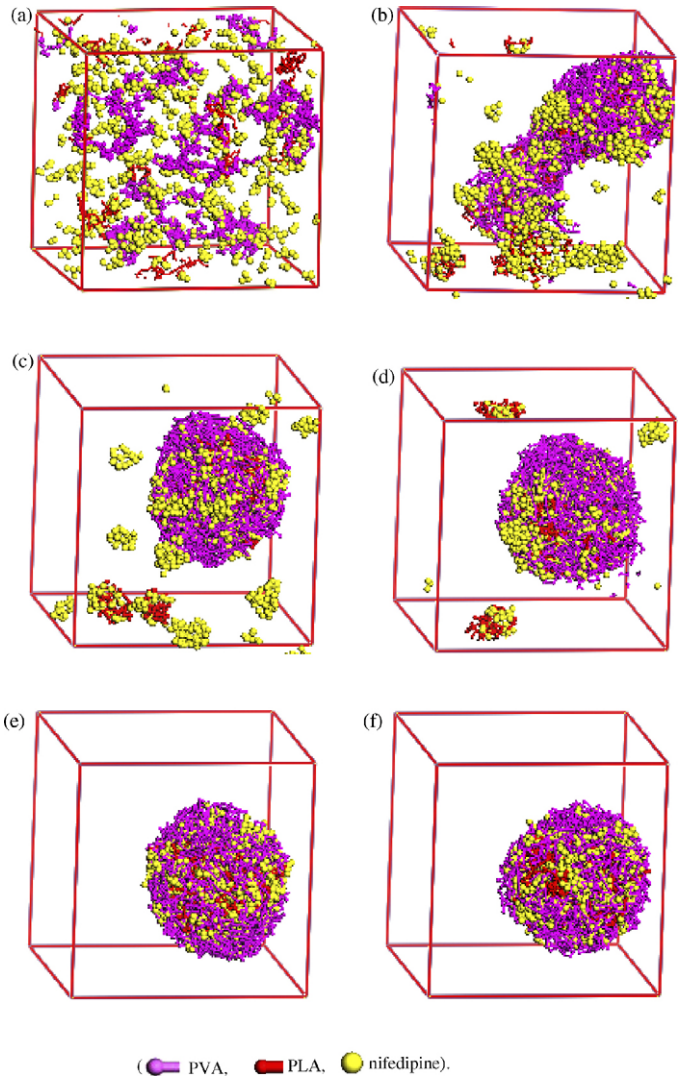

Fig. 2. Change of aggregates with increasing simulation steps. (a) 0 steps, (b) 1000 steps, (c) 2000 steps, (d) 5000 steps, (e) 20,000 steps, and (f) 30,000 steps. (PVA; PLA; nifedipine. (Legends of the beads are all same in the following figures as in this figure.)

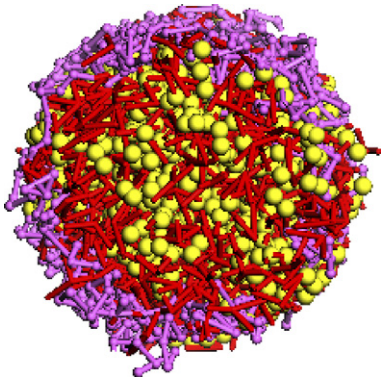

Fig. 3. Section view of one microsphere.

In Fig. 2a, all components are randomly mixed at the beginning of simulation. With the evolution of simulation (Fig. 2b and c), some PLA molecules aggregate and form clusters. Hydrophobic groups of amphiphilic PVA molecules adsorb around PLA clusters while hydrophilic groups of amphiphilic PVA molecules spread into the water phase. Therefore, PVA molecules distribute on the outer surface of PLA clusters, and spherical aggregates form. Many drug molecules still disperse in the water phase. PLA and drug molecules are both hydrophobic and are compatible with each other [24,25]. As simulation progresses, drug molecules gradually diffuse into the PLA matrix (Fig. 2c and d). At the simulation step of 20,000 (Fig. 2e), all drug molecules have dispersed into the PLA matrix, and a stable microsphere forms with stabilizer PVA molecules adsorbed on the outer surface of the PLA matrix. The aggregate morphology does not change significantly with extra simulation steps (Fig. 2f). All the following simulations are set to run 20,000 steps.

To observe the distribution of drug in PLA matrix more distinctly, a section view of one microsphere configuration at the simulation step of 20,000, is shown in Fig. 3. Drug molecules are amorphously and homogeneously distributed inside the PLA matrix. On the surface of the PLA matrix, hydrophobic groups (carbon chain) of PVA molecules are adsorbed, while hydrophilic groups (hydroxyl group) spread into water solution, resulting in a stable PLA microsphere.

3.2. Effect of the drug content on the aggregate morphology of DDS

The aggregate morphologies of DDS at different levels of drug contents are investigated. The molar ratio of PLA, PVA and water is fixed at 5:1:956. Results of simulation are shown in Fig. 4. A stable microsphere is observed with all drug molecules distributed inside the PLA matrix, which adsorbed by PVA molecules when drug content is low (Fig. 4a). With the increase of drug content, more and more drug molecules are distributed on the outer surface of the PLA matrix (Fig. 4b). When the molar ratio of the drug, PLA, and PVA increases to 37:5:1, the microsphere cannot encapsulate all drug molecules, and some small drug molecules form aggregates outside the microsphere, as shown in Fig. 4c. There is a maximum value for drug content that the PLA matrix can carry. The excess drug molecules will be repulsed outside the microsphere when the drug content exceeds the maximum. More and more drug molecules are repulsed outside the microsphere with the increase of drug content (Fig. 4d). When the molar ratio of the drug, PLA, and PVA is up to 80:5:1, the aggregate morphology of DDS is not a spherical structure any more, but a columnar structure with PVA molecules adsorbed on the outer surface (Fig. 4e). The aggregate morphology of DDS will be more complex and even be destroyed at higher drug content (Fig. 4f).

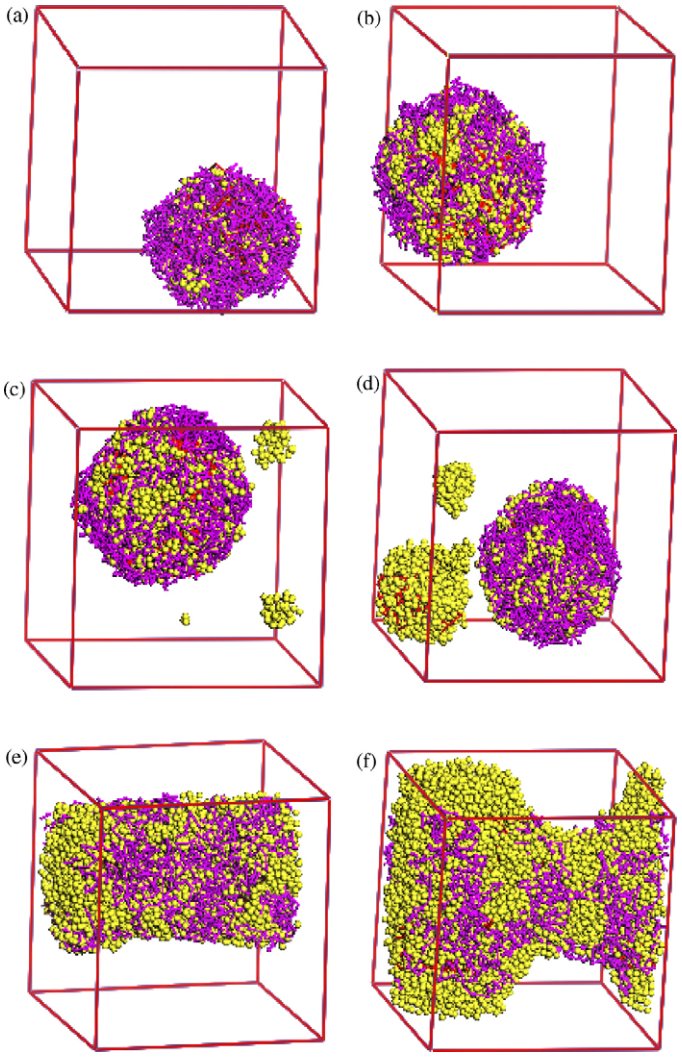

Fig. 4. Aggregate morphologies of DDS at different contents of drug. (a) 13:5:1:956, (b) 35:5:1:956, (c) 37:5:1:956, (d) 65:5:1:956, (e) 80:5:1:956, and (f) 103:5:1:956.

3.3. Effect of the PLA content on the aggregate morphology of DDS

The aggregate morphologies of DDS at different PLA contents are investigated also. In these simulations, the molar ratio of drug, PVA and water is fixed at 38:1:956. The results of simulations are shown in Fig. 5. The PLA matrix cannot carry all the drug molecules at a low content of PLA (Fig. 5a). Therefore some drug molecules are dispersed in the water phase, forming

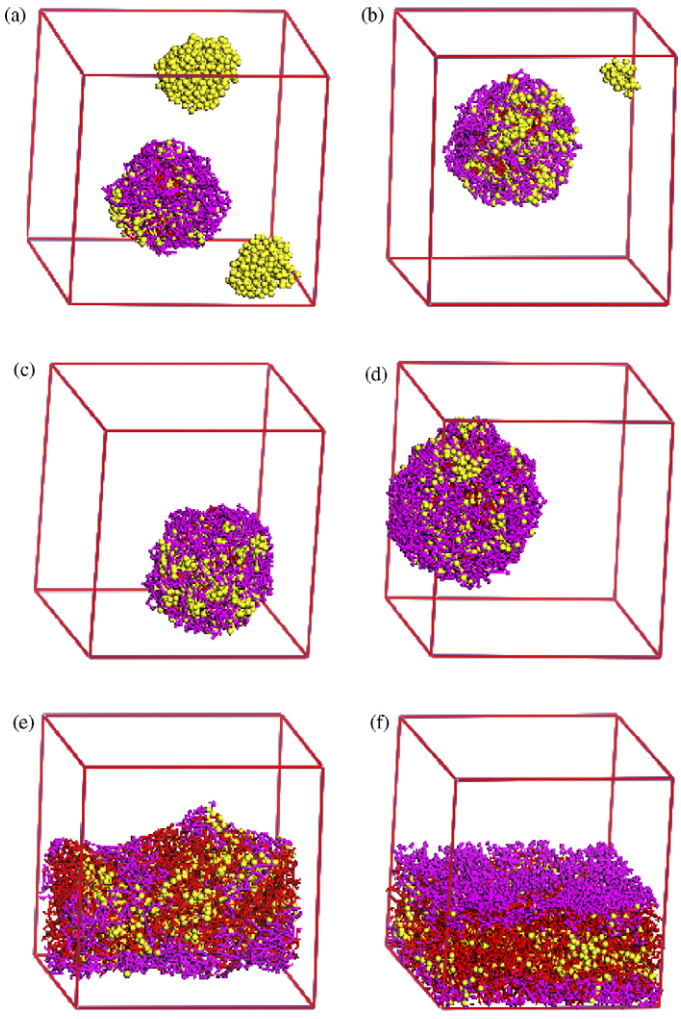

Fig. 5. Aggregate morphologies of DDS at different contents of PLA. (a) 38:1:1:956, (b) 38:4:1:956, (c) 38:5:1:956, (d) 38:7.5:1:956, (e) 38:8:1:956, and (f) 38:10:1:956.

drug aggregates. With the increase of PLA content, more drug molecules are distributed inside PLA matrix (Fig. 5b). When the molar ratio of the drug, PLA, and PVA approaches to 38:5:1, PLA matrix carries almost all drug molecules, resulting in a much more stable microsphere (Fig. 5c). The morphology of DDS does not change too much until the molar ratio of drug, PLA, and PVA is 38:7.5:1 (Fig. 5d). When the molar ratio of the drug, PLA, and PVA is up to 38:8:1, the aggregate morphology of DDS is a columnar structure, with PVA adsorbed on the outer surface (Fig. 5e). The columnar structure ensures a minimum contacting area of hydrophobic groups with water, so as to keep the system stable. A lamellar structure is gradually formed with the increase content of PLA (Fig. 5f).

3.4. Effect of the PVA content on the aggregate morphology of DDS

Variations of aggregate morphologies of DDS at different contents of PVA are shown in Fig. 6. As discussed above, PVA molecules play the key role of stabilization. When only a few PVA molecules are added to the solution, PLA clusters cannot be enwrapped completely, resulting in many unstable clusters (Fig. 6a). With the increase of PVA content, more PVA molecules are adsorbed outside the microsphere and less drug molecules are dispersed in water (Fig. 6b). When the molar ratio of drug, PLA, and PVA is up to 38:5:0.3, a stable microsphere forms with PVA molecules adsorbed on (Fig. 6c). When more PVA molecules are added to the solution, much smaller microspheres are obtained due to the surface tension (Fig. 6d). With the further increase of PVA content, columnar and lamellar structures are observed (Fig. 6e and f), because the density of polar groups distributed outside microspheres is higher and higher, which leads to stronger interactions among microspheres. Therefore, some of them contacted together to minimize the outer surface of microspheres and make the whole system more stable.

3.5. Effect of the water content on the aggregate morphology of DDS

The aggregate morphologies of DDS at different water contents are also investigated. The molar ratio of drug, PLA and

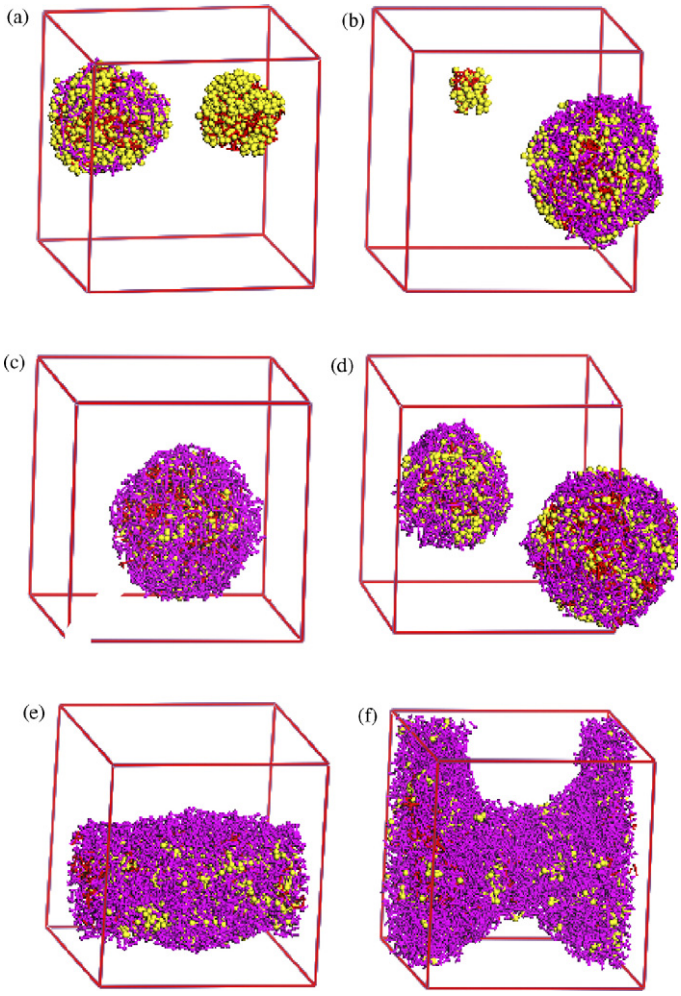

Fig. 6. Aggregate morphologies of DDS at different contents of PVA. (a) 38:5:0.1:956, (b) 38:5:0.2:956, (c) 38:5:0.3:956, (d) 38:5:2.2:956, (e) 38:5:2.5:956, and (f) 38:5:6:956.

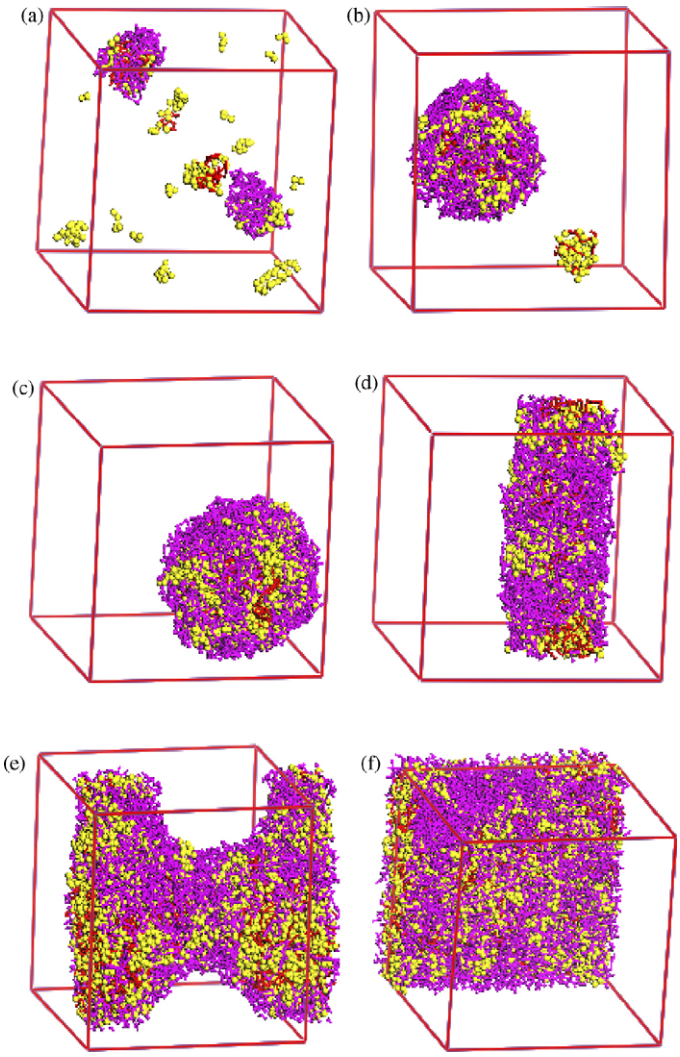

Fig. 7. Aggregate morphologies of DDS at different contents of water. (a) 38:5:1:5043, (b) 38:5:1:3528, (c) 38:5:1:665, (d) 38:5:1:643, (e) 38:5:1:610, and (f) 38:5:1:590.

PVA is fixed at 38:5:1. The results of simulations are shown in Fig. 7. The spherical structure could be hardly observed at the high content of water (Fig. 7a). This can be explained as large distances among oil molecules of drug, PLA, and PVA molecules. The interactions among them are too weak to make them aggregate. With the decrease of water content, oil molecules are closer and interactions among them are stronger. More and more oil molecules aggregate together, although some drug molecules are still dispersed in water (Fig. 7b). With the decrease of the molar ratio of drug, PLA, PVA and water, all drug molecules are distributed inside the PLA matrix with PVA molecules adsorbed upon the surface of the microsphere (Fig. 7c). When the molar ratio of drug, PLA, PVA and water decreased to 38:5:1:643, the aggregate morphology of DDS becomes columnar, which ensures a minimum contacting area of hydrophobic groups and water (Fig. 7d). A lamellar structure is formed when the content of water further decreased (Fig. 7e and f).

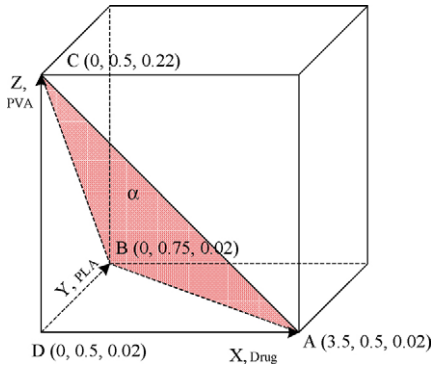

Fig. 8. Phase diagram for the formation of DDS microspheres.

3.6. Phase diagram of DDS for forming microspheres

Effects of different compositions on the forming of PLA microspheres have been studied by DPD simulations. The critical concentration of each component can be determined, which can be used to guide experiments. Firstly, the volume ratio of water phase to oil phase should be determined. Then, contents in the oil phase (containing PLA, drug, and PVA) should be further examined to ensure a spherical structure. It has been discussed in Section 3.5 that the molar ratio of drug, PLA, PVA, and water should be controlled between 38:5:1:665 and 38:5:1:3500 to guarantee a spherical structure of DDS. As all beads are assumed to have the same volume, therefore the volume ratio of water phase to oil phase can be replaced by the number ratio of beads in water phase to beads in oil phase. In DPD simulations, each molecule of drug, PLA, PVA and water is coarse-grained into beads with the bead number of 4, 55, 70 and 1, respectively. The lower limit of volume concentration of oil phase can be determined as:

$$\frac{38 \times 4 + 5 \times 55 + 1 \times 70}{(38 \times 4 + 5 \times 55 + 1 \times 70) + 3500 \times 1} = 12.4\%, \qquad (11)$$

Similarly, the upper limit can also be calculated as 42.8%. Thus, the volume concentration of the oil phase should be controlled at the interval of 12.4–42.8% to obtain spherical particles of DDS, that is:

$$12.4\% < 4X + 55Y + 70Z < 42.8\%, \qquad (12)$$

where X, Y and Z are the molar concentrations of drug, PLA, and PVA, respectively.

In the same way, concentrations of groups in oil phase can be determined from Sections 3.2–3.4 to obtain spherical particles of DDS. The range of the molar concentrations of drug, PLA and PVA are 0–3.5, 0.5–0.75, and 0.02–0.22%, respectively.

A coarse phase diagram for the formation of DDS microspheres has been proposed, as shown in Fig. 8. The plane α, enclosed by A, B, and C, shows the upper limit of composition of oil phase for the formation of microspheres. Bottom-left of plane α, i.e., the space closed by planes ABC, ABD, ACD and BCD is the domain which spherical structure of DDS could form. In the top-right space of plane α, spherical structures cannot be retained due to the high concentration of oil phase. In the space (ABCD) for the formation of DDS microspheres, the

space closer to *A* will result in a higher drug loading and lower encapsulation efficiency due to the high drug concentration. The space closer to *B* will cause larger mean size and higher encapsulation efficiency due to the high PLA concentrations. The space closer to *C* will result in smaller mean size, higher encapsulation efficiency and more stable microspheres, due to the high PVA concentration. Therefore, different compositions can be selected with different objectives. The described phase diagram could be used to guide the experimental preparation of DDS with desired properties.

4. Conclusions

DPD approach has been successfully applied to the investigation of composition effect on the formation of DDS microspheres. At a defined composition, the drug, PLA, and PVA could aggregate together and form microspheres in water phase. Drug molecules are amorphously and homogeneously distributed in PLA matrix. PVA molecules are adsorbed upon the surface of microspheres, acting as the stabilizer and the dispersant. Under different compositions, spherical, columnar, and lamellar structures have been observed. A phase diagram of DDS has been proposed, from which the recipe can be determined with different requirements. DPD simulations could not only provide insight into the mechanism of mesoscopic structures of DDS, but also serve as a complement to experiments and more efficiently guide the experimental preparation of DDS with desired properties.

Acknowledgements

Financial supports from the National Natural Science Foundation of China (No. 20476033, No. 20536020), and the China Excellent Young Scientist Fund (No. 20225620) are gratefully appreciated.

References

[1] S. Freiberg, X.X. Zhu, Polymer microspheres for controlled drug release, Int. J. Pharm. 282 (2004) 1–18.
[2] K.C. Wood, J.Q. Boedicker, D.M. Lynn, P.T. Hammond, Tunable drug release from hydrolytically degradable layer-by-layer thin films, Langmuir 21 (2005) 1603–1609.
[3] J.K. Vasir, K. Tambwekar, S. Garg, Bioadhesive microspheres as a controlled drug delivery system, Int. J. Pharm. 255 (2003) 13–32.
[4] E. Esposito, E. Menegatti, R. Cortesi, Hyaluronan-based microspheres as tools for drug delivery: a comparative study, Int. J. Pharm. 288 (2005) 35–49.
[5] S.K. Agrawal, N.S. Delong, J.M. Coburn, G.N. Tew, S.R. Bhatia, Novel release profiles from micellar solutions of PLA–PEO–PLA triblock copolymers, J. Control. Rel. 112 (2006) 64–71.
[6] S. Fischer, C. Foerg, S. Ellenberger, H.P. Merkle, B. Gander, One-step preparation of polyelectrolyte-coated PLGA microspheres and their functionalization with model ligands, J. Control. Rel. 111 (2006) 135–144.
[7] A.F. Carballido, R.H. Vanrell, I.T.M. Martínez, P. Pastoriza, Biodegradation ibuprofen-loaded PLGA microspheres for intraarticular administration effect of labrafil addition on release in vitro, Int. J. Pharm. 279 (2004) 33–41.
[8] P. Jie, S.S. Venkatraman, F. Min, B.Y.C. Freddy, G.L. Huat, Micelle-like nanoparticles of star-branched PEO–PLA copolymers as chemotherapeutic carrier, J. Control. Rel. 110 (2005) 20–33.
[9] A. Matsumoto, Y. Matsukawa, T. Suzuki, H. Yoshino, Drug release characteristics of multi-reservoir type microspheres with poly(DL-lactide-*co*-glycolide) and poly(DL-lactide), J. Control. Rel. 106 (2005) 172–180.
[10] P.J. Hoogerbrugge, J.M.V.A. Koelman, Simulating microscopic hydrodynamic phenomena with dissipative particle dynamics, Europhys. Lett. 19 (3) (1992) 155–160.
[11] J.M.V.A. Koelman, P.J. Hoogerbrugge, Dynamic simulations of hard-sphere suspensions under steady shear, Europhys. Lett. 21 (3) (1993) 363–368.
[12] P. Español, P. Warren, Statistical mechanics of dissipative particle dynamics, Europhys. Lett. 30 (4) (1995) 191–196.
[13] R.D. Groot, P.B. Warren, Dissipative particle dynamics: bridging the gap between atomistic and mesoscopic simulation, J. Chem. Phys. 107 (11) (1997) 4423–4435.
[14] R.D. Groot, T.J. Madden, Dynamic simulation of diblock copolymer microphase separation, J. Chem. Phys. 108 (20) (1998) 8713–8724.
[15] R.D. Groot, Mesoscopic simulation of polymer–surfactant aggregation, Langmuir 16 (2000) 7493–7502.
[16] R.D. Groot, Electrostatic interactions in dissipative particle dynamics-simulation of polyelectrolytes and anionic surfactants, J. Chem. Phys. 118 (24) (2003) 11265–11277.
[17] R.D. Groot, K.L. Rabone, Mesoscopic simulation of cell membrane damage, morphology change and rupture by non-ionic surfactants, Biophys. J. 81 (2) (2001) 725–736.
[18] S.L. Yuan, Z.T. Cai, G.Y. Xu, Y.S. Jiang, Mesoscopic simulation study on phase diagram of the system oil/water/aerosol OT, Chem. Phys. Lett. 365 (2002) 347–353.
[19] A. Maiti, S. McGrother, Bead–bead interaction parameters in dissipative particle dynamics: relation to bead-size, solubility parameter, and surface tension, J. Chem. Phys. 120 (3) (2004) 1594–1601.
[20] Y.M. Li, G.Y. Xu, Y.X. Luan, S.L. Yuan, Z.Q. Zhang, Studies on the interaction between tetradecyl dimethyl betaine and sodium carboxymethyl cellulose by DPD simulations, Colloids Surf. A 257–258 (2005) 385–390.
[21] R.E.V. Vliet, H.C.J. Hoefsloot, P.D. Iedema, Mesoscopic simulation of polymer–solvent phase separation: linear chain behavior and branching effects, Polymer 44 (2003) 1757–1763.
[22] S.L. Yuan, G.Y. Xu, Y.X. Luan, C.B. Liu, The interaction between polymer and AOT or NaDEHP in aqueous solution: mesoscopic simulation study and surface tension measurement, Colloids Surf. A 256 (2005) 43–50.
[23] C.X. Long, L.J. Zhang, Y. Qian, Mesoscale simulation of drug molecules distribution in the matrix of solid lipid microparticles (SLM), Chem. Eng. J. 119 (2006) 99–106.
[24] L.J. Zhang, C.X. Long, J.Z. Pan, Y. Qian, A dissolution-diffusion model and quantitative analysis of drug controlled release from biodegradable polymer microspheres, Can. J. Chem. Eng. 84 (2006) 556–558.
[25] J.Z. Pan, L.J. Zhang, Y. Qian, Structure–property relationships and models of controlled drug delivery of biodegradable poly(D,L-lactic acid) microspheres, Chin. J. Chem. Eng. 12 (6) (2004) 869–876.
[26] H.J. Qian, Z.Y. Lu, L.J. Chen, Z.S. Li, C.C. Sun, Dissipative particle dynamics study on the interfaces in incompatible A/B homopolymer blends and with their block copolymers, J. Chem. Phys. 122 (2005) 184907.
[27] S. Yamamoto, S.A. Hyodo, Mesoscopic simulation of the crossing dynamics at an entanglement point of surfactant threadlike micelles, J. Chem. Phys. 122 (2005) 204907.
[28] F.L. Dong, Y. Li, P. Zhang, Mesoscopic simulation study on the orientation of surfactants adsorbed at the liquid/liquid interface, Chem. Phys. Lett. 399 (2004) 215–219.